Polymer 50 (2009) 2451–2459

Contents lists available at ScienceDirect

Polymer

journal homepage: www.elsevier.com/locate/polymer

Dilute solutions and phase behavior of polydisperse A-*b*-(A-*co*-B) diblock copolymers

Daniel Gromadzki*, Jan Lokaj, Miroslav Šlouf, Petr Štěpánek

Institute of Macromolecular Chemistry, Academy of Sciences of the Czech Republic, Heyrovsky Sq. 2, 162 06 Prague 6, Czech Republic

ARTICLE INFO

Article history:
Received 15 December 2008
Received in revised form
27 February 2009
Accepted 17 March 2009
Available online 24 March 2009

Keywords:
Diblock copolymer
Dilute solution properties
Microphase separation

ABSTRACT

The effect of polydispersity on dilute solution properties and microphase separation of polydisperse high-molecular-weight ($M_w > 10^5$ g mol^{-1}) polystyrene-*block*-poly(styrene-*co*-acrylonitrile) diblock copolymers, PS-*block*-P(S-*co*-AN), was studied in this work. For experiments, a series of diblock copolymers with variable weight fractions of acrylonitrile units ($w_{AN} = 0.08$–0.29) and length of block P(S-*co*-AN) was synthesized using nitroxide-mediated radical polymerization (NMP) technique, namely, by chain extension of nitroxide-terminated polystyrene (PS-TEMPO). According to light scattering and viscometry measurements in dilute tetrahydrofuran (THF) solutions the studied diblock copolymers assumed random coil conformation with the values of characteristic structure factor $R_g/R_h = 1.50$–1.76. It was found that polydisperse diblock copolymers being in strong segregation limit (SSL) self-assembled into microphase-separated ordered morphologies at ordinary temperature. The long periods of lamellar microdomains were larger compared to theoretical predictions for hypothetical monodisperse diblock copolymers. It was demonstrated by means of SAXS and TEM that a transition from a lamellar (LAM) to irregular face-centered-cubic (FCC) morphology occurred with increasing volume fraction of P(S-*co*-AN) block.

1. Introduction

Diblock copolymers A-*b*-B are known for their ability to self-assemble into a variety of ordered morphologies on the nanometer length scale via the process of microphase separation [1]. In dilute solutions of non-selective solvents theoretical and experimental results indicate a preferential ordering (segregation) of chemically dissimilar segments in a diblock copolymer due to unfavorable thermodynamic interactions governed by the Flory–Huggins segmental interaction parameter χ_{AB} and the volume fraction (Φ) of the respective blocks. There are also other models suggesting a diblock copolymer consisting of two mutually interpenetrating random coils in an expanded conformational state [2]. In solutions containing non-selective solvents and A-*b*-B diblock copolymers, the diffusion processes were identified and thoroughly studied by many authors [3–6]. In bulk, the characteristic self-assembled morphologies (body-centered-cubic spheres (S), cylindrical (C), lamellar (L), complex bicontinuous gyroid structure (G)) were predicted by Leibler in the framework of a mean-field theory (MFT) [7] and subsequently extended to include fluctuation effects by Fredrickson [8–10].

In contrast to ionically prepared diblock copolymers A-*b*-B, much less information both on solution and bulk or thin layer morphologies can be found in the literature for systems of A-*b*-(A-*co*-B) diblock copolymers produced by recently discovered controlled/living radical polymerization (CRP) methods [11]. Block copolymers prepared by these polymerization schemes can have considerable polydispersities (PDI), yet they exhibit propensity to self-assemble into array of periodic morphologies [12,13]. According to mean-field theoretical predictions [14–16] PDI can influence the ordered phase behavior such as the domain spacing and the resultant morphology to a great extent. Lynd explored this effect by designing a diblock copolymer poly(ethylene-*alt*-propylene)-*b*-poly(DL-lactide) (PEP-PLA), in which ionically prepared PEP block was kept constant while the PDI of PLA block formed by ring-opening polymerization were systematically varied at fixed overall average composition and number-average molecular weight M_n [17,18]. They found that the lamellar spacing increased with the increase in PDI (PDI varied from 1.2 to 2) supporting previous theoretical predictions. More recently, Listak et al. investigated polystyrene-*b*-poly(methyl acrylate) copolymer (PS-PMA), with approximately symmetric molecular weight distribution (MWD) synthesized using activators regenerated by electron transfer

* Corresponding author. Tel.: +420 2 96809296; fax: +420 2 96809410.
E-mail address: d_grom@interia.pl (D. Gromadzki).

0032-3861/$ – see front matter © 2009 Elsevier Ltd. All rights reserved.
doi:10.1016/j.polymer.2009.03.022

(ARGET) for atom transfer radical polymerization (ATRP). It allowed to conveniently control MWD by adjusting the amount of copper catalyst. The resulting polydisperse PS-PMA copolymers formed highly ordered hexagonally perforated lamellar (HPL) morphology. The authors demonstrated that the skewness of the distribution of block molecular weights is an important parameter influencing microphase separation process [19]. Yet, in a very recent work Mueller et al. reported on the polydispersity-induced stabilization of core–shell gyroid morphology [20] and made it clear that polydispersity can be a useful tool for controlling phase behavior and morphological transitions in block copolymers.

Shortly after the publishing of nitroxide-mediated radical polymerization (NMP) technique [21], Fukuda et al. reported the synthesis of polystyrene-*block*-poly(styrene-*co*-acrylonitrile) diblock copolymers [22]. Specifically, TEMPO-terminated polystyrene macroinitiator was used as macroinitiator in the copolymerization of an azeotropic mixture of styrene (S) and acrylonitrile (AN). Indeed, in contrast to anionic polymerization [23] CRP methods such as NMP [24], ATRP [25] and reversible addition-fragmentation chain transfer (RAFT) [26] offer the possibility to polymerize various monomers in a statistical fashion [27]. The Fukuda's approach was subsequently extended by other workers and diblock copolymers with a higher fraction of acrylonitrile in the statistical block, P(S-*co*-AN) [28,29], have been prepared. We have adopted a slightly different strategy for the synthesis of these diblock copolymers by NMP, namely, chain extension of TEMPO-terminated poly(styrene-*co*-acrylonitrile) macroinitiators with styrene; in addition, preparation of polystyrene-*block*-poly(styrene-*co*-acrylonitrile)-*block*-polystyrene (A-*b*-(A-*co*-B)-*b*-A) triblock copolymers has been reported [30,31].

To our knowledge neither the dilute solution properties nor the effect of polydispersity on the microphase separation behavior was previously discussed for diblock copolymers A-*b*-(A-*co*-B) therefore we wish to address this issue in the present paper.

2. Experimental section

2.1. Materials

Dibenzoyl peroxide (Bz_2O_2), 2,2,6,6-tetramethylpiperidin-1-yloxy radical (TEMPO), styrene (S), acrylonitrile (AN), tetrahydrofuran (THF), *N*,*N*-dimethylformamide (DMF) and methanol were purchased from Aldrich Co. The monomers were distilled before use. Solvents were of analytical grade.

2.2. Synthesis of diblock copolymers

2.2.1. Synthesis of polystyrene-block-poly(styrene-co-acrylonitrile) diblock copolymers

Polystyrene-*block*-poly(styrene-*co*-acrylonitrile) diblock copolymers, PS-*block*-P(S-*co*-AN), were synthesized by nitroxide-mediated radical polymerization. First, styrene was polymerized at 125 °C using an initiating system Bz_2O_2/TEMPO under formation of a TEMPO-capped polystyrene (PS-TEMPO) (Table 1). The PS-TEMPO was subsequently employed as macroinitiator in the S–AN copolymerization at different mole ratios of the comonomers in the feed. Diblock copolymers A1–A5 were obtained from the initial mixtures with the mole ratio of S/AN equal to 80/20, 63/37 (azeotropic composition), 40/60 and 20/80, respectively.

2.3. Samples preparation

2.3.1. Preparation of the polymer solutions for light scattering measurements

All samples for light scattering measurements were prepared by direct dissolution of certain amount of the polymer in the organic solvent and the resulting solutions were gently stirred overnight to ensure complete dissolution of the polymer. After the dissolution step, samples were filtered through suitable Millipore filters with pore sizes of 0.45 μm and flame sealed in a light scattering cell.

Table 1
Characteristics of PS-TEMPO macroinitiator and related PS-*block*-P(S-*co*-AN) diblock copolymers (A1–A5).

Polymer	$M_n \times 10^{-4}$ [a]	M_w/M_n	f_{S1}	f_{AN}	(f_{AN})
PS-TEMPO	4.44	1.10	1	–	–
A1	9.03 (10.28)	1.38	0.40	0.15	0.25
A2	12.34 (15.32)	1.45	0.25	0.28	0.37
A3	14.80 (21.21)	1.57	0.17	0.38	0.45
A4	11.40 (14.45)	1.54	0.25	0.38	0.51
A5	9.07 (24.87)	1.51	0.14	0.44	0.51

f_{S1} is the mole fraction of styrene units from the PS-TEMPO macroinitiator, incorporated in the diblock copolymer, f_{AN} and (f_{AN}) are the mole fractions of acrylonitrile units in the diblock copolymer and in the attached poly(styrene-*co*-acrylonitrile) block, respectively.

[a] Polystyrene-equivalent molecular weight determined by SEC; the values in parentheses were calculated from equation (3).

2.3.2. Preparation of the diblock copolymer membranes for SAXS and TEM

Membranes from diblock copolymers PS-*block*-P(S-*co*-AN) were prepared by solution casting technique. Typically, 5 mL of a THF solution (8 wt%/v) was poured into a Petri dish (3 cm in diameter and 1.3 cm in height) and let slowly to evaporate at room temperature for one week. Some of the membranes were subsequently subjected to thermal annealing at the temperature above 160 °C for at least 12 h in vacuum to achieve the equilibrium morphology.

2.4. Characterization techniques

2.4.1. Size exclusion chromatography

Molecular weights of polymers were estimated using SEC instrument: Deltachrom pump (Watrex Comp.), autosampler Midas (Spark Instruments, The Netherlands), two columns with PL gel MIXED-B LS (10 μm), separating in the range of molecular weights approximately $400–1 \times 10^7$ g mol^{-1}. Evaporative light scattering PL-ELS-1000 (Polymer Laboratories) was used as detector. THF was the mobile phase, flow rate was 0.5 mL/min. The injection-loop volume was 0.1 mL. Polystyrene reference standards in the range $4000–1.6 \times 10^6$ were used for the calibration of the system. Some measurements were performed with triple viscosity/concentration/light-scattering detection. The set was connected to a light-scattering photometer DAWN DSP-F (Wyatt Technology Corp.), measuring at 18 angles of observation, a modified differential viscometer Viscotek model TDA 301 (without internal light scattering and concentration detectors) and a differential refractometer Shodex RI 71. The data were accumulated and processed using the Astra and triSec software. The evaluation of the triple-detection data is described elsewhere [32].

2.4.2. Viscosity determination of dilute polymer solutions

Viscosity measurements were performed using Ubbelohde capillary viscometers adapted for subsequent dilution. The flow times were recorded opto-electrically using a home-made apparatus. The temperature was kept constant at 25 ± 0.01 °C. The dimensions of viscometers were such that viscometric corrections were negligible. The concentration was chosen so that the relative viscosity η_r (i.e., ratio t/t_0 of flow times of solution and solvent) was between 1.1 and 1.8.

Intrinsic viscosity [η] was obtained using Huggins equation (1)

$$\eta_{sp}/c = [\eta] + k_H[\eta]^2 c + \cdots \quad (1)$$

where k_H is the Huggins constant obtained from the slope of the linear dependence of η_{sp}/c *vs.* c, $\eta_{sp} = (\eta_r - 1)$; η_{sp} is the specific viscosity and η_r is the relative viscosity.

2.4.3. Light scattering measurements

THF solutions of diblock copolymers have been investigated by dynamic light scattering (DLS) using an ALV instrument equipped with a 22 mW He–Ne laser in the angular range 30–150°. The measured intensity correlation curves $g^2(t)$ were converted into distributions $A(\tau)$ of relaxation times τ using the inverse Laplace transformation

$$g^2(t) = 1 + \beta\left[\int A(\tau)\exp(-t/\tau)d\tau\right]^2 \quad (2)$$

where t is the delay time of the correlation function and β an instrumental parameter. The programme REPES [33] was used to perform the inverse Laplace transformation in Eq. (2). The relaxation time τ is related to the translational diffusion coefficient D by the relation $D = (\tau q^2)^{-1}$ where q is the scattering vector. The hydrodynamic radius R_h of the particles is calculated from D using the Stokes–Einstein equation

$$D = k_B T/6\pi\eta_0 R_h \quad (3)$$

where T is absolute temperature, η_0 the viscosity of the solvent and k_B the Boltzmann constant. By a similar procedure, the distribution of relaxation times $A(\tau)$ can be transformed into a distribution of hydrodynamic radii $A(R_h)$.

Static light scattering measurements were performed on the same ALV instrument in the angular range $\theta = 30$–150°, and temperature 25 °C. The apparatus was calibrated with toluene as a standard. The processed data are represented as

$$Kc/\Delta R(\theta, c) = (M_w P(\theta))^{-1} + 2A_2 c + \cdots \quad (4)$$

where M_w is the weight-average molecular weight; K is the optical constant which includes the square of the refractive index increment dn/dc; $\Delta R(\theta)$ is the excess Rayleigh ratio, proportional to the intensity of light scattered from solutions, A_2 is the second virial coefficient, and c is the polymer concentration in g mL^{-1}.

The refractive index increment (dn/dc) of the diblock copolymer was measured with the Brice–Phoenix differential refractometer at $\lambda = 632.8$ nm in THF.

Some experiments were performed on a Zetasizer Nano-ZS, Model ZEN3600 (Malvern Instruments, UK). For evaluation of data, the DTS (Nano) program was used.

2.4.4. Small-angle X-ray scattering (SAXS)

Small-angle X-ray scattering was used to examine the morphology of synthesized diblock copolymers in bulk before and after thermal annealing. Experiments were performed using a pinhole camera (Molecular Metrology SAXS System) attached to a microfocused X-ray beam generator (Osmic MicroMax 002) operating at 45 kV and 0.66 mA (30 W). The camera was equipped with a multiwire, gas-filled area detector with an active area diameter of 20 cm (Gabriel design). Two experimental setups were used to cover the q range of 0.007–1.1 Å^{-1} ($q = (4\pi/\lambda)\sin\theta$, where λ is the wavelength and 2θ is the scattering angle). The scattering intensities were put on absolute scale using a glassy carbon standard. The thickness of as-cast and thermo-annealed films was measured by digital micrometer and was in the range of 120–200 μm, however, for SAXS experiment several pieces were stacked to get thickness of 1000–2000 μm.

2.4.5. Transmission electron microscopy (TEM)

TEM measurements were performed on a microscope JEM 200CX (Jeol, Japan) or Tecnai G2 Spirit (FEI, Czech Republic). All microphotographs were taken at acceleration voltage 100 kV (JEM 200CX) or 120 kV (Tecnai G2) and recorded with a digital camera. Brightness, contrast and gamma corrections were performed with standard software. Ultrathin sections of ca. 50 nm were cut from the thermo-annealed bulk sample with the ultramicrotome Leica Ultracut UCT, equipped with cryo attachment. Temperatures during cutting were −110 °C and −50 °C for the sample and the knife, respectively. The samples were stained with the vapor of RuO_4 to obtain contrast images.

3. Results and discussion

3.1. Synthesis of diblock copolymers

The chemical structure of diblock copolymers under study is depicted in Fig. 1.

In the diblock copolymers, the mole fractions of both styrene units, f_{S1} from the macroinitiator and comonomer units, f_{S2}, f_{AN} from the formed S–AN copolymer block, were determined as follows:

a) Using the published monomer reactivity ratios, $r_S = 0.49$ and $r_{AN} = 0.04$ [34], the S–AN copolymerization diagram was constructed. For a given feed, the corresponding mole fractions of comonomer units in the resulting S–AN copolymer, (f_S) and (f_{AN}), were found.
b) The mole fraction f_{AN} was determined from nitrogen analysis or ^{1}H NMR.
c) The mole fraction f_{S2} was calculated according to equation (5):

$$f_{S2} = f_{AN} \times (f_S)/(f_{AN}) \quad (5)$$

d) The mole fraction f_{S1} was expressed by equation (6):

$$f_{S1} = 1 - (f_{S2} + f_{AN}) \quad (6)$$

Polystyrene-equivalent molecular weights were measured by SEC. Unimodal eluograms (not shown), indicating the complete consumption of the PS-TEMPO macroinitiator, were observed. The M_n values of diblock copolymers were therefore calculated also according to equation (7) [31]

$$M_n = 4.44 \times 10^4[1 + f_{S2}/f_{S1} + (f_{AN} \times M_{AN})/(f_{S1} \times M_S)]; \quad (7)$$

4.44×10^4 is the number-average molecular weight of PS-TEMPO, f_{S1}, f_{S2} and f_{AN} correspond to the above-mentioned mole fractions, M_S and M_{AN} are molecular weights of S and AN, respectively.

The results of GPC analysis and composition of the synthesized polymers are summarized in Table 1.

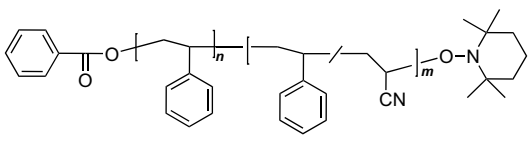

PS-*block*-P(S-*co*-AN)-TEMPO

Fig. 1. Chemical formulae of studied diblock copolymers polystyrene-*block*-poly(styrene-*co*-acrylonitrile) (PS-*block*-P(S-*co*-AN)-TEMPO).

Table 2
Molecular characteristics of PS-TEMPO macroinitiator and related diblock copolymers determined by triSEC.

Polymer	$M_n \times 10^{-4}$ (g mol^{-1})	$M_w \times 10^{-4}$ (g mol^{-1})	M_w/M_n	R_g[a] (nm)	$c^*_{R_g}$[b] (%)	R_g[c] (nm)	R_h[d] (nm)	ρ[e]	w_{PS}[f]	w_{AN}[g]
PS-TEMPO	4.10	5.62	1.37	9.7	1.8	10.7	6.3	1.70	1	–
A1	7.65	13.10	1.71	16.0	1.2	16.2	10.4	1.55	0.53	0.080
A2	10.13	17.71	1.75	19.2	1.0	19.1	12.7	1.50	0.40	0.165
A3	10.10	18.51	1.83	19.7	0.66	22.3	14.5	1.53	0.40	0.236
A4	10.34	17.59	1.70	19.1	0.69	21.6	12.6	1.71	0.39	0.242
A5	14.35	26.48	1.84	24.4	0.56	26.6	15.1	1.76	0.28	0.290

[a] Radius of gyration estimated using relation established for PS in benzene.
[b] Size related cross-over concentration estimated using values of R_g measured by triSEC.
[c] Experimental values of radius of gyration.
[d] Hydrodynamic radius.
[e] Dimensionless parameter $\rho = R_g/R_h$.
[f] w_{PS} – weight fraction of neat polystyrene block.
[g] w_{AN} – weight fraction of acrylonitrile units in the diblock copolymer (from elemental analysis).

The discrepancy between measured and calculated M_n for diblock copolymers A3, A4 and especially A5 with higher fraction of acrylonitrile units is large; this is due to inability of SEC calibrated with PS-standards to distinguish between different nature of incorporated comonomer units. Therefore, the measured molecular weights represent only the apparent values.

3.2. Dilute solution properties in THF

The absolute values of molecular weight M_n and M_w and molecular parameters, i.e., radius of gyration, R_g, and hydrodynamic radius, R_h, for all diblock copolymers were determined by triSEC setup equipped with the triple light-scattering, viscosity and concentration detection in THF and are listed in Table 2.

All studied diblock copolymers are well soluble in THF despite the fact that it is thermodynamically good solvent for polystyrene but a very bad solvent for polyacrylonitrile [35]. SLS measurements on A5 diblock copolymer containing the highest fraction of AN ($w_{AN} = 0.29$) were performed to verify the results from triSEC analysis and obtain qualitative information about the polymer–solvent interactions (second osmotic virial coefficient, A_2). Two independent SLS experiments were done using Malvern and ALV instruments allowing the values of M_w, A_2 and R_g to be determined by the Zimm mode (see Table 3).

The values of both radius of gyration $R_g = 26.6$ nm and $R_g = 26$ nm and weight-average molecular weight, $M_w = 264.8 \times 10^3$ g mol^{-1} and $M_w = (260 \pm 20) \times 10^3$ g mol^{-1}, for A5 diblock copolymer measured by triSEC and Malvern at 25 °C, respectively, are in excellent agreement. The positive value of $A_2 = (6.7 \pm 0.3) \times 10^{-4}$ cm^3 mol g^{-2} also shows that THF is still a good solvent for A5 copolymer.

It is tempting to compare the experimental values of R_g for diblock copolymers in THF with those for linear polystyrene homopolymer in benzene using relation [36,37]

$$R_g = 1.45 \times 10^{-9} M^{0.595} \text{ [cm]} \quad (8)$$

It was previously shown that benzene being a good solvent for PS exhibits comparable solvating power to THF and ethylbenzene [38].

Table 3
Molecular characteristics of diblock copolymer A5 obtained by SLS measurements in THF at 25 °C.

Parameter	Values
$M_w \times 10^{-3}$ (g mol^{-1})	260 ± 20
A_2, $\times 10^{-4}$ (cm^3 mol g^{-2})	6.7 ± 0.3
R_g (nm)	26
dn/dc (mL g^{-1})	0.141

A_2 – second virial coefficient.
dn/dc – refractive index increment.

The estimated values of radii of gyration for PS standard ($R_g = 9.7$ nm) in benzene and the experimental one for neat PS-TEMPO macroinitiator ($R_g = 10.7$ nm) and corresponding diblock copolymers A1 and A2 (see Table 2 for comparison) with relatively low fraction of acrylonitrile units are in a very good agreement. A difference arises once a higher fraction of acrylonitrile has been incorporated into the statistical block of A3–A5 diblock copolymers with values of R_g slightly larger in THF compared to PS/benzene system. This difference follows a different trend than one expects from knowledge of solvent quality suggesting that the amount of acrylonitrile monomers in P(S-*co*-AN) block is not sufficient to induce coil shrinkage or forcing the diblock copolymer to self-organize into micellar structure. Indeed, coil shrinkage or micelle formation is ruled out by the dimensionless parameter defined as the ratio of the static to dynamic radii $\rho = R_g/R_h$ which was determined for all polymer samples (see Table 2). It was frequently reported that ρ index is a sensitive measure of macromolecular architecture and conformation in solution [39]. For micelles (homogeneous hard sphere) the value is predicted to be 0.778 [39] while for linear PS in a good solvent system ρ was usually found at 1.50 in accord with renormalization group (RG) calculations for nondraining chains [40,41]. A significant scatter of the latter value exists in literature [41]. We found $\rho = 1.70$ for PS macroinitiator which is substantially larger compared to RG predictions and very different from $\rho = 1.30$ for monodisperse PS standard in THF reported by Bhatt and Jamieson [42]. It seems therefore that polydispersity of the studied PS/THF solution is a main factor influencing ρ. To support this conclusion, Park et al. [43] found from light scattering measurements that any peculiar behavior exists in solutions of nearly monodisperse polystyrenes in good solvents – THF, toluene and carbon tetrachloride – suggesting that the conformation of PS in these three solvents can be well described by RG parameters [44]. For the full series of diblock copolymers studied the generalized ratio was in the range $\rho = 1.50$–1.76 which is a parameter describing a flexible coil in a good solvent [39].

The predictions of diffusion behavior for random and block copolymers appear to be far more complex compared to pure homopolymers because of the heterogeneities in monomers' distribution along the copolymer chain. The distribution of styrene and acrylonitrile in the second P(S-*co*-AN) block of A3 diblock copolymer has nearly random arrangement since it was prepared at azeotropic composition. The remaining diblock copolymers are characterized by substantial polydispersities in molar masses and composition. Despite this fact, diblock copolymer A5 was further investigated by dynamic light scattering in order to fully elucidate the effect of incorporated AN units on the solution properties. First, the critical concentration (overlap or cross-over concentration), $c^*_{R_g}$, was estimated using relation (9) [37] (see Table 2).

$$c^*_{R_g} = M_w/(4/3)\pi N_A R_g^3 \quad (9)$$

Another definition of cross-over concentration c^* providing a good thermodynamic definition for the chain overlap is second virial coefficient-related overlap concentration $c^*_{A_2} = (A_2 M_w)^{-1}$. Using values of M_w, A_2 we get $c^*_{A_2} = 0.57\%$ which is in a perfect agreement with previously determined value $c^*_{R_g} = 0.56\%$. DLS is a particularly suitable technique to study the dynamics and diffusion processes of high-molecular-mass polymers and is not influenced by the presence of low-molecular-mass impurities [45]. Angular DLS measurements were performed on polymer solutions at five concentrations from $c = 1 \times 10^{-3}$ g mL^{-1} to $c = 1 \times 10$ g mL^{-1}. The measured relaxation rates ($\Gamma = 1/\tau$) *vs.* q^2 for two representative concentrations are plotted in Fig. 2. The relation $\Gamma = Dq^2$ was satisfied for all solution concentrations and the least-square fit to the slope of the straight lines gives the translational diffusion coefficients D.

The translational diffusion coefficient D was then used to calculate hydrodynamic radii of isolated polymer chains applying the Stokes–Einstein relation (7). These values are compiled in Table 4.

Fig. 3 shows dependence of translation diffusion coefficients as a function of concentration for A5 diblock copolymer in THF at 25 °C.

For dilute polymer solutions the concentration dependence of the translational diffusion coefficient can be expressed as

$$D(c) = D_0(1 + k_D c + \cdots) \quad (10)$$

where c is the polymer concentration and D_0 is the diffusion coefficient at infinite dilution.

Linear least-square extrapolation was performed to obtain D_0 from the intercept, and the value of the parameter k_D from the slope. Generally, positive values of k_D are found in good solvents and negative values are found in Θ solvents. In other words, the thermodynamic effect outweighs the friction effect and the diffusion coefficient increases with concentration. Mes et al. [45] found similar dependence of k_D for polydisperse P(S-*co*-AN) copolymers in THF. There are several methods in the literature for estimating diffusion coefficient of homopolymers at infinite dilution [46]. We have neglected for a moment factors related to monomer arrangement and chemical heterogeneities discussed above and used equation derived by Johnston and Rudin [47]

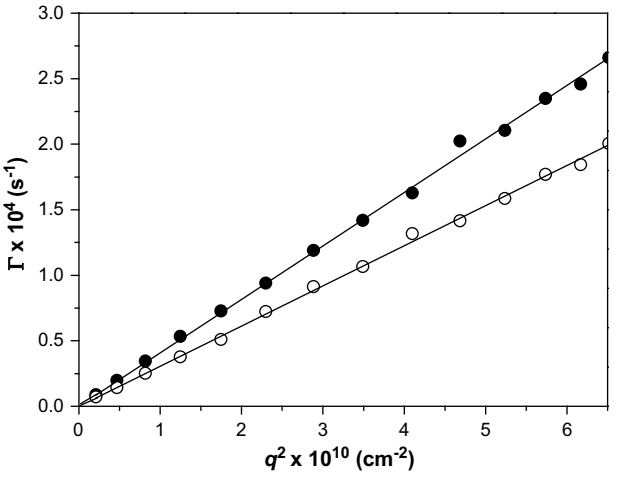

Fig. 2. Dependence of Γ on q^2 for a dilute solution ($c = 1 \times 10^{-3}$ g mL^{-1}) of diblock copolymer A5 ($M_w = 264.8 \times 10^3$ g mol^{-1}) in THF (open circles) and in the vicinity of the overlap concentration c^* (closed circles). The measurements were performed in the angular range from 20° to 150°. The solid lines represent the linear fits to the experimental data. The translational diffusion coefficients D were obtained from fits to the slopes.

Table 4
Translational diffusion coefficient D and hydrodynamic radii R_h for A5 diblock copolymer in THF at various concentrations.

$c \times 10^{-3}$ g mL^{-1}	$D(c) \times 10^{-7}$ (cm^2 s^{-1})	R_h (nm)
1	3.06	16.1
3	3.07	15.6
5	3.32	14.4
7	3.55	13.6
10	4.00	12.0

$$D_0 = \frac{kT}{6\pi\eta_0}\left(\frac{10\pi N_A}{3K_v M_v^{a+1}}\right) \quad (11)$$

where k is Boltzmann constant, T is the absolute temperature, N_A is Avogadro's number, η_0 is the viscosity of the solvent, and M_v is the viscosity-average molecular weight. The parameters K_v and a are Mark–Houwink–Kuhn–Sakurada constants (the polymolecularity correction factor for polymers with $M_w/M_n = 1.7$ is negligible) established by light scattering for polystyrene in the molecular weight range of 13,000 and 2.2×10^6 g mol^{-1} in THF at 25 °C [48]. The theoretical value of $D_0 = 2.2 \times 10^{-7}$ cm^2 s^{-1} estimated by Johnston's method seems to be in reasonable agreement with the experimental $D_0 = 2.8 \times 10^{-7}$ cm^2 s^{-1}. The concentration dependent diffusion coefficient $k_D = 38.01 \pm 0.01$ mL g^{-1} for studied A5 diblock copolymer in THF was found to be in a very good agreement with data of Duval and Hadziioannou [49] for PS of similar M_w in THF and in reasonable agreement with literature value $k_D = 31.4 \pm 3.6$ mL g^{-1} [50] for polydisperse random copolymers P(S-*co*-AN) of similar molecular weight in DMF (good solvent for PS and AN). In contrast, theoretical predictions of Yamakawa [46]

$$k_D(y) = 0.8A_2M - (N_A V_h/M) - \bar{v} \quad (12)$$

(where $\bar{v}$ is the partial specific volume of the polymer in the solvent determined by density measurements and $V_h = 4/3\pi R_h^3$) yielded much larger value $k_D = 100$ mL g^{-1} compared to experimental one. At infinite dilution $D(c)$ is influenced by both thermodynamic and hydrodynamic interactions and can be expressed by the relation between k_D and concentration dependent friction coefficient k_f [51]

$$k_D = 2A_2M - k_f - \bar{v} \quad (13)$$

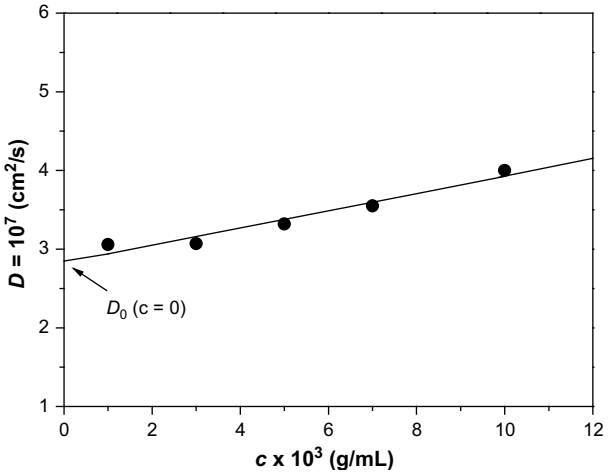

Fig. 3. Translational diffusion coefficients obtained by DLS as a function of concentration for A5 diblock copolymer in dilute THF at 25 °C.

The value of $k_f = 314\ \mathrm{mL\,g^{-1}}$ obtained here was again compared with value reported in ref. [51] and found to be approximately two times higher than PS/THF system and almost six times higher compared to values for linear polyisobutylene in chloroform (good solvent) [41]. This behavior can be presumably assigned to difference in draining character: AN monomers are much less solvated that PS chain sequences and the draining effect is therefore larger for AN than for PS.

The value of hydrodynamic radius $R_h = 16.1$ nm ($c = 1 \times 10^{-3}\ \mathrm{g\,mL^{-1}}$) is very close to corresponding apparent thermodynamic radius $R_{A_2} = 16.6$ nm calculated from relation

$$R_{A_2} = \left(3M^2A_2/16\pi N_A\right)^{1/3} \tag{14}$$

The dimensionless ratio R_{A_2}/R_h is 1.03 which is in excellent agreement with theoretical estimates for linear polymers in a good solvent [41].

Measurement of intrinsic viscosity for A5 diblock copolymer in THF at 25 °C yields value $[\eta] = 85\ \mathrm{cm^3/g}$ which is not very different from $[\eta] = 96\ \mathrm{cm^3/g}$ estimated according to Appelt and Meyerhoff experimental relation [52]

$$[\eta] = 1.363 \times 10^{-2} M_w^{0.71}\ \left(\mathrm{cm^3\ g^{-1}}\right) \tag{15}$$

for PS homopolymer of the same molecular weight.

The viscometric radius, R_η, was determined based on the equation for hard spheres [39]

$$R_\eta = \left(3/10\pi N_A\right)^{1/3}\left([\eta]M_w\right)^{1/3} \tag{16}$$

This value $R_\eta \approx 15.2$ nm together with $R_h \approx 16$ nm determined by DLS in a dilute THF solution yields generalized ratio of $R_\eta/R_h = 0.95$ which is slightly lower than unity usually found for linear and branched structures in a good solvent [53]. According to Burchard both radii R_h and R_η reflect interaction of macromolecule with the solvent and have different physical definition, the latter being influenced by shear gradient field. Mays et al. [54] suggested that R_η/R_h ratios may assume larger values for a given polymer in thermodynamically moderate solvent compared to good or Θ solvent. The lack of corresponding literature references and theoretical predictions for R_η/R_h values prevents us from further speculations.

In the following the static and hydrodynamic parameters are explored within RG theory which predicts specific values for certain universal ratios [55–57]

$$\psi = A_2M^2/4\pi^{3/2}N_AR_g^3 \tag{17}$$

$$U_{A\eta} = A_2M/[\eta] \tag{18}$$

$$U_{f_s} = f/R_g\eta_0 \tag{19}$$

$$U_{\eta s} = M[\eta]/N_AR_g^3 \tag{20}$$

in which f represents friction expressed as $f = 6\pi\eta_0R_f = kT/6\pi\eta_0D_0$.

The values of universal ratios along with previously discussed generalized ratios for A5 diblock copolymer are shown in Table 5.

Table 5
Generalized and universal ratios for A5 diblock copolymer in THF.

	R_g/R_h	R_{A_2}/R_h	R_η/R_h	ψ	U_{f_s}	$U_{\eta s}$	$U_{A\eta}$
Theory	1.56	–	1.12	0.22	12.07	4.08	1.19
PS	1.52	–	0.98	–	–	–	–
A5	1.76	1.03	0.95	0.18	11.38	1.96	2.07

For sake of comparison, listed in Table 5 are also results predicted by theory and values for monodisperse PS in THF.

Unfortunately, the latter data in the molecular weight range relevant to our case were mostly unavailable in work of Venkataswamy et al. [44]. They found disagreement of universal ratios with RG theory in THF of PS in a wide range of molecular weight investigated, though data in ethylbenzene agreed very well with theoretical predictions. The generalized ratios R_g/R_h and R_η/R_h are proportional respectively to U_{f_s} and $U_{\eta s}$. The values of ψ, U_{f_s} derived from static parameters for A5 in THF are in a very good agreement with RG theory. Although there is a less good agreement with theoretical predictions in values $U_{\eta s}$ and $U_{A\eta}$, the difference remains in an acceptable range.

3.3. Phase behavior of PS-block-P(S-co-AN) diblock copolymers in the melt state

Diblock copolymers PS-*block*-P(S-*co*-AN) investigated in this work formed optically transparent films indicating absence of macrophase separation despite the broad molecular weight distribution. The equilibrium state and a specific microphase-separated morphology of a diblock copolymer A-*b*-B is determined by the overall degree of polymerization, N, the composition, i.e., the volume fraction of A segment with respect to segment A and B and the Flory–Huggins interaction parameter, χ_{AB} [58], between both segments expressed as $\chi_{AB} = (a/T) + b$, where T is the absolute temperature and a and b are constants for the particular A–B monomer pair. The order–disorder transition (ODT) occurs at a critical value of the product $\chi_{AB}N$ which determines the equilibrium thermodynamic melt state behavior of a particular diblock copolymer. The Flory–Huggins interaction parameter was estimated according to

$$\chi_{AB} = \frac{\upsilon}{RT}(\delta_A - \delta_B)^2 \tag{21}$$

where υ is an average monomer volume, δ_A and δ_B are the solubility parameters of polymers A and B, respectively, and R is the gas constant. For an average monomer volume of $100\ \mathrm{cm^3/mol}$, $\delta_{PS} = 18.2\ (\mathrm{J/cm^3})^{1/2}$ and $\delta_{AN} = 28.4\ (\mathrm{J/cm^3})^{1/2}$ this yields an interaction parameter $\chi_{S/AN} = 4.16$ at room temperature which is several times higher compared to literature value $\chi_{S/AN} \cong 0.8$ [59]. Note, that conditions, i.e., temperature and solubility parameters (this depends on method of measurement) for estimation of the reference value [59] were not reported which makes direct comparison impossible. It is, however, known that due to a large difference in

Table 6
Characteristics of diblock copolymers obtained by SAXS analysis.

Diblock copolymer	N[a]	$\chi_{S/AN}N$	Φ_{PS}[b]	Morphology	d (nm)[c]	d (nm)[d]
A1	744	3095	0.53	LAM	126 (103)	60
A2	1018	4235	0.40	LAM	139 (110)	74
A3	1041	4330	0.39	LAM	131 (116)	75
A4	1071	4455	0.38	LAM	130 (121)	77
A5	1529	6360	0.27	FCC	74 (64)	–

[a] Total degree of polymerization of the diblock copolymer.
[b] Volume fraction of neat PS block calculated from molecular weight and mass density values of S and AN 1.05 g cm^{-3} and 0.81 g cm^{-3}, respectively.
[c] Interdomain spacing extracted from the first maximum q^* of the log–log scattering curve using Bragg relation for LAM and C lattice structure $d = 2\pi/q_o$ and $d = (1/q_o)(4\pi/3)$, respectively. The more accurate values given in parentheses were obtained after applying first-order correction procedure. For samples exhibiting LAM phase the intensities were multiplied through by q^2 (Lorenz correction) while A5 sample exhibiting C ordering was multiplied through by q to account for the form factor of individual lamellae or spheres on the scattering intensity $I(q)$ [61].
[d] Hypothetical interlamellar spacing for monodisperse diblock copolymer estimated based on Semenov's SSL theory [63].

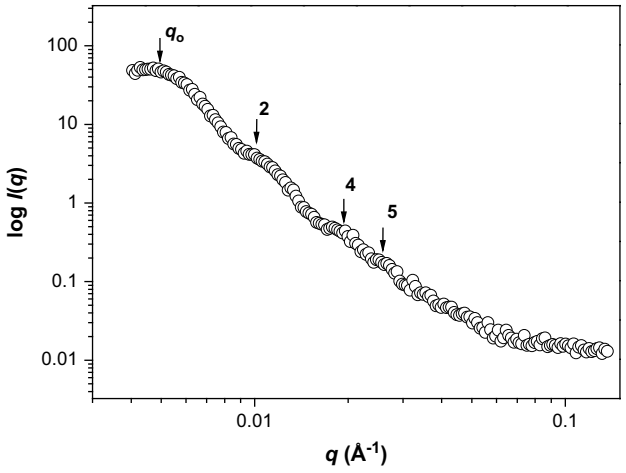

Fig. 4. SAXS pattern obtained on diblock copolymer A4 cast from THF and thermo-annealed at 160 °C for at least 12 h with indicated positions of multiple scattering diffractions.

cohesive energy density between S and AN monomer pair with the values of binary segmental contact energy parameters $\delta_{S/AN} = 45.1$ J/cm^3 [60] the highly unfavorable intersegmental interaction is often referred to as the intramolecular repulsion effect. The presence of 36–43 wt% styrene in the statistical block is expected to have a minor effect on segregation strength and phase behavior. This is understood based on simple group contribution calculations discussed by Ruzette [13] for styrene/acrylic/methacrylic systems applying well-known random copolymer effect. The phase behavior of block copolymers studied here can be mapped out knowing the volume fraction of one component Φ and the degree of incompatibility defined as a product $\chi_{S/AN}N$. The former values were estimated from absolute molecular weight and the density of styrene and acrylonitrile 1.05 and 0.81 g cm^{-3}, respectively. The data are listed in Table 6.

The values of product $\chi_{S/AN}N$ greatly exceed $\chi N \approx 100$ which means that considered block copolymers are in strong segregation limit (SSL). Leibler's MFT predicts a second-order phase transition from the disordered to the lamellar phase at the critical point $(\chi N)_{ODT} = 10.5$ for a diblock copolymer with a symmetric composition. Based on these rough estimations one shall expect formation of lamellar morphology for nearly symmetric A1–A4 diblock copolymers while for A5 sample a cubic (C) type lattice. SAXS analysis was first performed on all films cast from THF solutions in order to obtain these information and the size of microphase-separated domains. SAXS diffractograms (not shown) recorded for A1–A3 diblock copolymers exhibited only a first maximum corresponding to the characteristic dimension of the microphase-separated structure (see Table 6). In contrast, scattering curves of diblock copolymers A4 (see Fig. 4), A5 (not shown), besides clear first maximum, revealed presence of several higher order side maxima. This effect is due to a larger fraction of acrylonitrile in studied copolymer which increases the difference in average electron density between monomers. A4 and A5 diblock copolymers contain similar overall weight fraction of acrylonitrile $w_{AN} = 0.24$ and $w_{AN} = 0.29$ but different volume fraction of a neat PS first block, $\Phi_S = 0.38$ and $\Phi_S = 0.27$, therefore these samples were further characterized by SAXS and TEM. Analysis of the scattering curve for A4 diblock copolymer reveals lamellar microdomain ordering with scattering maxima at q ratios 1:2:4:5 (indicated by arrows in the plot), superposed to interface scattering from the grains (Porod law). This superposition and the presence of defects in the lamellar structure can explain that the expected odd-order Bragg reflection 3 is not seen on the scattering pattern. The absence of multiple and sharp diffraction maxima of the studied samples indicates liquid-like order of microdomains which is in contrast to our previous work on similar diblock copolymers of lower molecular weights and narrower MWDs [31].

Fig. 5 shows TEM micrograph on thin sections of solution cast A4 diblock copolymer without any treatments (A) and on the same diblock after thermal annealing at 160 °C overnight (B). Both images display reasonably well-ordered lamellar microstructures. The slight deformation of the lamellae on thermo-annealed sample might be explained by the preparation procedure and cut of the ultrathin specimens.

TEM image (Fig. 5A) of as-cast A4 diblock copolymer film shows well-separated lamellar domains, namely RuO_4-stained polystyrene phase which appears dark on the photograph and grey regions of P(S-*co*-AN) block. After thermal treatment (image B) one can see appearance of white and grey regions in the middle and at the edges of lamellae, respectively. Obviously, an increase in

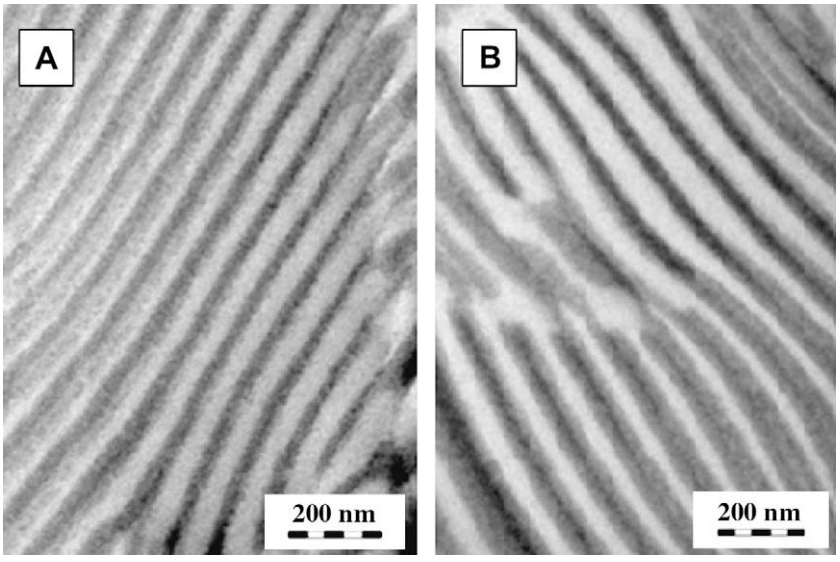

Fig. 5. TEM micrograph of as-cast A4 (A) and after thermal annealing at 160 °C for at least 12 h (B).

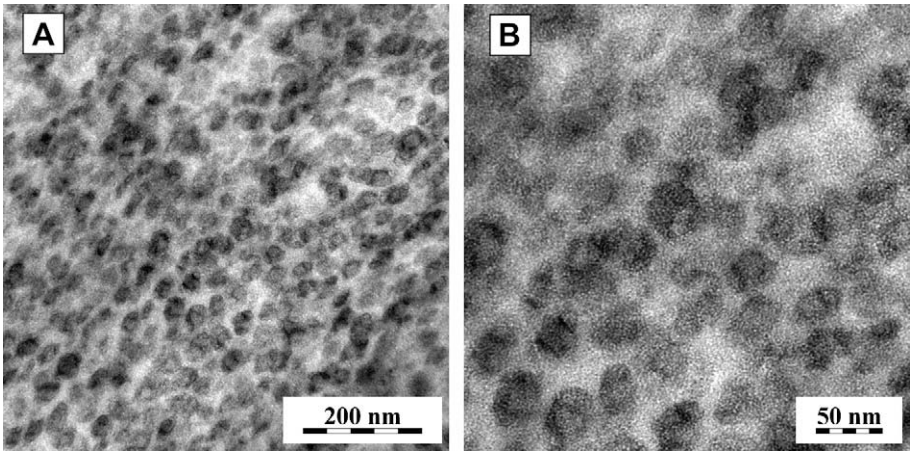

Fig. 6. TEM micrographs of the neat A5 diblock copolymer (A) and the same A5 sample with higher magnification (B).

temperature favors inter-mixing of PS and P(S-*co*-AN) blocks resulting in enhanced segregation of respective styrene-rich and acrylonitrile-rich phases. At the annealing temperature the Flory–Huggins interaction parameter $\chi_{S/AN} = 2.89$ is lower compared to $\chi_{S/AN} = 4.16$ at room temperature. The characteristic interlamellar spacing d calculated using the program imageJ [62] on TEM images for as-cast and thermo-annealed A4 sample yields value, $d = 136$ nm and $d = 130$ nm, respectively. The latter value is in excellent agreement with $d = 131$ nm for thermo-annealed sample inferred from first-order Bragg reflection ($q_o = 0.0048$ Å^{-1}) of the SAXS scattering curve using equation $d = 2\pi/q_o$. For strongly segregated diblock copolymers the lamellar period is expected to scale with $N^{2/3}$ and depends only weakly on the χ parameter. The experimentally found lamellar period can be compared to a value predicted for a hypothetical model monodisperse block copolymer of equivalent N according to strong segregation theory [63]

$$d = \frac{4}{\sqrt{6}}\left(\frac{3}{\pi^2}\right)^{1/3} aN^{2/3}\chi^{1/6} \tag{22}$$

where a is the average statistical segment (Kuhn) length which was taken as average between PS (6.7 Å) and AN (7.2–7.68 Å) [34,64]. The theoretical lamellar periods (60–77 nm) for A1–A4 diblock copolymers listed in Table 6 (last row) are correspondingly lower compared to Lorentz-corrected values (103–121 nm) extracted from SAXS. These results are consistent with theoretical predictions [14,65] and experimental results [13,17,18] obtained recently by other authors and clearly illuminate the effect of polydispersity on the long period of microphase-separated lamellar structure. For A5 diblock copolymer a transition from lamellar to strongly disordered cubic phase is observed with increasing volume fraction of P(S-*co*-AN) which is supported by the corresponding TEM image shown in Fig. 6A. PS-rich domains appearing as dark spheres on the micrograph are embedded in a continuous matrix of P(S-*co*-AN) and are only locally arranged into face-centered-cubic (FCC) lattice as visualized by TEM micrograph taken at higher magnification (Fig. 6B). The reason for lack of long-range order is not the sample history, i.e., the fact that this membrane was not subjected to thermal annealing (as-cast A4 exhibits well-ordered lamellar morphology suggesting that phase behavior depends on the segregation strength of the material; see Fig. 5) but it is certainly the effect of considerably increased polydispersity.

It is recognized that CRP mediated by TEMPO is not suitable for acrylonitrile and (meth)acrylate type monomers unless certain amount of styrene is present in the polymerization mixture to retain the instantaneous concentration of propagating radicals and suppress irreversible termination events. Let us recall that A5 diblock copolymer was prepared starting from PS-TEMPO at the monomer composition S/AN 20/80, i.e., with majority of AN in the feed. A faster consumption of styrene at early stages of chain extension and considerable increase in viscosity of polymerization medium (polyacrylonitrile is not soluble in its monomer) are the factors which contributed to a loss of control and significant increase in polydispersity.

4. Conclusions

Hydrodynamic and thermodynamic parameters were determined for styrenic diblock copolymers containing AN units in dilute THF solutions and compared with literature data on the neat polystyrene in THF and other good non-selective solvents. Based on the vast quantity of static and dynamic data accumulated in this work, it was concluded that THF remained thermodynamically as a good solvent for diblock copolymers PS-*b*-P(S-*co*-AN) despite a rather large content (up to 29 wt%) of AN units incorporated in the random block. Both TEM and SAXS experiments demonstrated that polydisperse PS-*b*-P(S-*co*-AN) diblock copolymers spontaneously self-assembled into lamellar and strongly disordered face-centered-cubic morphologies in the melt. Formation of ordered morphologies depends exclusively on volume fraction of one of the block. This implies that a diblock copolymer in which first block is composed of PS and the second one is a mixture of S and AN from thermodynamic point of view behaves as a classical diblock copolymer [66]. The long periods of the resulting microphase-separated lamellar phases were larger compared to hypothetical monodisperse analog of the same molecular weight $d = 126$–139 nm and $d = 60$–77 nm, respectively.

Acknowledgements

The authors acknowledge Dr. P. Holler and Dr. M. Netopilík for results of elemental and SEC analyses, respectively. Dr. J. Pleštil is acknowledged for X-ray scattering data, and Dr. J. Horský for viscosity measurements. We thank Drs. J. Holoubek and Č. Koňak for reading the manuscript and their comments on this work. The authors gratefully acknowledge support by the Grant Agency of the Czech Republic (SON/06/E005) within the EUROCORES Programme SONS of the European Science Foundation, which is also supported by the European Commission, Sixth Framework Programme. D.G. gratefully acknowledges support within MCRTN-SOCON (Marie Curie Fellowship; contract No MCRTN-CT-2004-512331).

References

[1] Hamley IW, editor. The physics of block copolymers. 1st ed. Oxford University Press; 1998.
[2] Gromadzki D, Filippov S, Netopilík M, Makuška R, Jigounov A, Pleštil, J. et al. Combination of "living" nitroxide-mediated and photoiniferter-induced "grafting from" free-radical polymerizations: from branched copolymers to unimolecular micelles and microgels. Eur Polym J, in press, doi:10.1016/j.eurpolymj.2009.02.022.
[3] Balsara NP, Štěpánek P, Lodge TP, Tirrell M. Macromolecules 1991;24:6227.
[4] Pan C, Maurer W, Liu Z, Lodge TP, Štěpánek P, von Meerwall ED, et al. Macromolecules 1995;28:1643.
[5] Liu Z, Kobayashi K, Lodge TP. J Polym Sci Part A Polym Phys 1998;36:1831.
[6] Duval M, Haida H, Lingelser JP, Gallot Y. Macromolecules 1991;24:6867.
[7] Leibler L. Macromolecules 1980;13:1602.
[8] Fredrickson GH, Helfand E. J Chem Phys 1987;87:697.
[9] Barrat JL, Fredrickson GH. J Chem Phys 1991;95:1281.
[10] Bates FS, Fredrickson GH. Annu Rev Phys Chem 1990;41:525.
[11] Gaynor S, Greszta D, Mardare D, Teodorescu M, Matyjaszewski K. J Macromol Sci Pure Appl Chem 1994;31:1561.
[12] Bendejacq D, Ponsinet V, Joanicot M, Loo YL, Register RA. Macromolecules 2002;35:6645.
[13] Ruzette AV, Girault ST, Leibler L, Chauvin F, Bertin D, Guerret O, et al. Macromolecules 2006;39:5804.
[14] Leibler L, Benoit H. Polymer 1981;22:195.
[15] Burger C, Ruland W, Semenov AN. Macromolecules 1991;24:816.
[16] Sides SW, Fredrickson GH. J Chem Phys 2004;121:4974.
[17] Lynd NA, Hillmyer MA. Macromolecules 2005;38:8803.
[18] Lynd NA, Hillmyer MA. Macromolecules 2007;40:8050.
[19] Listak J, Jakubowski W, Mueller L, Plichta A, Matyjaszewski K, Bockstaller MR. Macromolecules 2008;41:5919.
[20] Mueller AJ, Ellison CJ, Hillmyer MA, Bates FS. Macromolecules 2008;41:6272.
[21] Georges MK, Veregin RPN, Kazmaier PM, Hamer GK. Macromolecules 1993;26:2987.
[22] Fukuda T, Terauchi T, Goto A, Tsujii Y, Miyamoto T, Shimizu Y. Macromolecules 1996;29:3050.
[23] Baskaran D, Müller AHE. Prog Polym Sci 2007;32:173.
[24] Hawker CJ, Bosman AW, Harth E. Chem Rev 2001;101(12):3661.
[25] Braunecker WA, Matyjaszewski K. Prog Polym Sci 2007;32:93.
[26] Moad G, Rizzardo E, Thang SH. Polymer 2008;49(5):1079.
[27] Matyjaszewski K, Gnanou Y, Leibler L, editors. Macromolecular engineering: from precise macromolecular synthesis to macroscopic materials properties and applications. Weinheim: Wiley-VCH; 2007.
[28] Baumert M, Mülhaupt R. Macromol Rapid Commun 1997;18:787.
[29] Baumann M, Roland AI, Schmidt-Naake G, Fischer H. Macromol Mater Eng 2000;280:1.
[30] Lokaj J, Brozova L, Holler P, Pientka Z. Collect Czech Chem Commun 2002; 67:267.
[31] Gromadzki D, Lokaj J, Černoch P, Diat O, Nallet F, Štěpánek P. Eur Polym J 2008;44:189.
[32] Gromadzki D, Makuška R, Netopilík M, Holler P, Lokaj J, Janata M, et al. Eur Polym J 2008;44:59.
[33] Jakeš J. Collect Czech Chem Commun 1995;60:1781.
[34] Brandrup J, Immergut EH, Grulke EA, editors. Polymer handbook. 4th ed. New York: Wiley; 1999.
[35] Mullik SU, Norrish RGW. Proc R Soc Lond 1975;344:1.
[36] de Gennes PG. Scaling concepts in polymer physics. Ithaca, NY: Cornell University Press; 1979.
[37] Adam M, Delsanti M. Macromolecules 1977;10:1229.
[38] Jamieson AX, Venkataswamy K. Polym Bull 1984;12:275.
[39] Burchard W. Adv Polym Sci 1999;143:113.
[40] Appelt B, Meyerhoff G. Macromolecules 1980;13:657.
[41] Brown W, Zhou P. Macromolecules 1991;24:5151.
[42] Bhatt M, Jamieson AM. Macromolecules 1998;21:3015.
[43] Park S, Chang T, Lee JW, Pak H. Bull Korean Chem Soc 1991;12:682.
[44] Venkataswamy K, Jamieson AM, Petschek RG. Macromolecules 1986;19:124.
[45] Mes EP, Kok WTH, Poppe H, Tijssen R. J Polym Sci Polym Phys 1999;37:593.
[46] Yamakawa H. Modern theory of polymer solutions. New York: Harper and Row; 1971 [chapter 6].
[47] Johnston HK, Rudin A. J Polym Sci Polym Lett Ed 1971;9(55):84.
[48] Benoit H, Grubisic Z, Rempp P, Decker D, Zillox J. J Chem Phys 1996;63:1507.
[49] Hadziioannou G, Cotts PM, ten Brinke G, Han CC, Lutz P, Strazielle C, et al. Macromolecules 1978;20:493.
[50] Raju K, Blanks RF. J Polym Sci Polym Phys Ed 1979;17:583–95.
[51] Vrentas JS, Duda JL. J Appl Polym Sci 1976;20:2569.
[52] Neyerhoff G, Appelt B. Macromolecules 1979;12:968.
[53] Roovers J, Martin JE. J Polym Sci Polym Phys Ed 1989;27:2513.
[54] Mays JW, Nan S, Lewis ME. Macromolecules 1991;24:4857.
[55] Oono Y, Kohomoto M. J Chem Phys 1983;78:520.
[56] Douglas JF, Freed KF. Macromolecules 1984;17:2344.
[57] Douglas JF, Freed KF. Macromolecules 1984;17:2354.
[58] Flory PJ. Principles of polymer chemistry. Ithaca, NY: Cornell University Press; 1953.
[59] Kroeze E, ten Brinke G, Hadzioannou. Polymer 1997;38:379.
[60] Yang Q, Mao Y, Li G, Huang Y, Tang P, Lei C. Mater Lett 2004;58:3939.
[61] Russell TP. In: Brown GS, Moncton DE, editors. Handbook on synchrotron radiation, vol. 3. New York: North-Holland; 1991. p. 379.
[62] National Institute of Health. Available from: <http://rsb.info.nih.gov/ij/>.
[63] Semenov AN. Sov Phys JETP 1985;61:733.
[64] Gonzales C, Zamora F, Guzmán. J Macromol Sci Phys B 1987;26:257.
[65] Burger C, Ruland W, Semenov AN. Macromolecules 1990;23:3339.
[66] Gromadzki D, Černoch P, Janata M, Kudela V, Nallet F, Diat O, et al. Eur Polym J 2006;42:2486.